



HAL
open science

3-Amido-benzo[b]silines: straightforward modular 2-step synthesis and photophysical properties

Stéphane Golling, Tiahong Yan, Valérie Mazan, Frédéric Leroux, Ilaria Ciofini, Morgan Donnard

► **To cite this version:**

Stéphane Golling, Tiahong Yan, Valérie Mazan, Frédéric Leroux, Ilaria Ciofini, et al.. 3-Amido-benzo[b]silines: straightforward modular 2-step synthesis and photophysical properties. *Advanced Synthesis and Catalysis*, In press, 10.1002/adsc.202400293 . hal-04538289

HAL Id: hal-04538289

<https://hal.science/hal-04538289>

Submitted on 19 Apr 2024

HAL is a multi-disciplinary open access archive for the deposit and dissemination of scientific research documents, whether they are published or not. The documents may come from teaching and research institutions in France or abroad, or from public or private research centers.

L'archive ouverte pluridisciplinaire **HAL**, est destinée au dépôt et à la diffusion de documents scientifiques de niveau recherche, publiés ou non, émanant des établissements d'enseignement et de recherche français ou étrangers, des laboratoires publics ou privés.



Distributed under a Creative Commons Attribution - NonCommercial 4.0 International License

3-Amido-benzo[*b*]silines: Straightforward Modular 2-Step Synthesis and Photophysical Properties

Stéphane Golling,^a Tianhong Yan,^b Valérie Mazan,^a Frédéric R. Leroux,^a Ilaria Ciofini,^b and Morgan Donnard^{a,*}

^a Université de Strasbourg, CNRS, Université de Haute-Alsace
LIMA – UMR 7042

ECPM, 25 rue Becquerel, 67000 Strasbourg – France

E-mail: donnard@unistra.fr

^b Chimie ParisTech, PSL University, CNRS,

Institute of Chemistry for Life and Health Sciences, Theoretical Chemistry and Modeling Team

75005 Paris, France

Manuscript received: March 16, 2024; Revised manuscript received: March 23, 2024;

Version of record online: ■■, ■■■



Supporting information for this article is available on the WWW under <https://doi.org/10.1002/adsc.202400293>

Abstract: In this manuscript we report the synthesis of 3-amido-benzo[*b*]silines thanks to a 2-step strategy involving a 3-component silylformylation of ynamides followed by a Friedel-Crafts cyclization/isomerizing dehydration domino sequence. This reaction is tolerant to various structural variations and has allowed us to synthesize a library of diversely substituted silacycles with yields from 33 to 85%. We also studied the fluorescence properties of these compounds which show structural similarities with recognized probes such as Si-Rhodamine for example.

Keywords: Silacycles; Benzosiline; Fluorescence; Silylformylation; Ynamide

Introduction

Silacycles, referring to silicon-based heterocycles, have gained significant attention in recent years for their potential use in various fields such as materials, medicine, electronics and fragrances.^[1] As a single example, it is well established now that the C/Si switch can modulate beneficially the pharmacokinetic parameters of various drugs (different biodistribution, better stability towards metabolic pathways, modulation of non-covalent *in vivo* molecular interactions).^[2] However, one of the main limits to a more extensive use of such scaffolds is the restricted number of synthetic methodologies available. Consequently, intensive work has been done over the last two decades to access various families of silacycles, with silole derivatives as the first focus.^[1] Although less studied, 6-membered ring silacycles, *i.e.* the siline derivatives, have demonstrated their very high potential as biomaging fluorescent probes^[3] and in drug design^[2] (Figure 1.a). These applications are particularly identified for benzosiline-based scaffolds. Notably, the available synthesis strategies are much less abundant in comparison to

siloles and are essentially focused on the synthesis of, mainly symmetrical, dibenzosilines (silanthracene derivatives) thanks to the double nucleophilic attack of diaryl lithium species on dichlorosilanes (Figure 1.b-I).^[4] However, over the last 15 years, several groups have focused their efforts on developing new approaches involving modern metal catalysis to these specific silacycles. These strategies include, non-exhaustively, intramolecular^[5] or intermolecular^[6] ring expansion of silacyclobutanes^[7] (Figure 1.b-II), metal-catalyzed ring closing reaction of silicon tethered partners, such as ring-closing metathesis (RCM),^[8] intramolecular C–H activation^[9] or radical cyclization^[10] (Figure 1.b-III), and finally intramolecular silylation reactions on alkenes or alkynes (Figure 1.b-IV).^[11]

Although often highly effective, these approaches are generally limited in terms of the structural variations possible around silylated heterocycles and, for most of them, require several synthesis steps to obtain the substrates, which further limits the possibilities for rapid structural variations required in the case

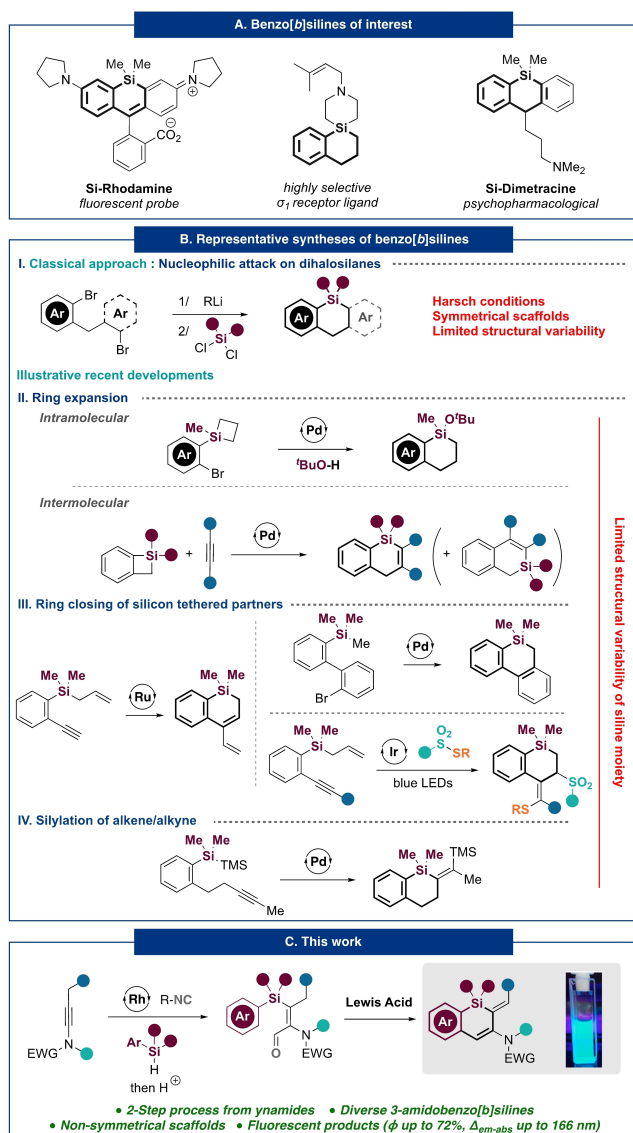


Figure 1. Contextualization of the work reported in this manuscript.

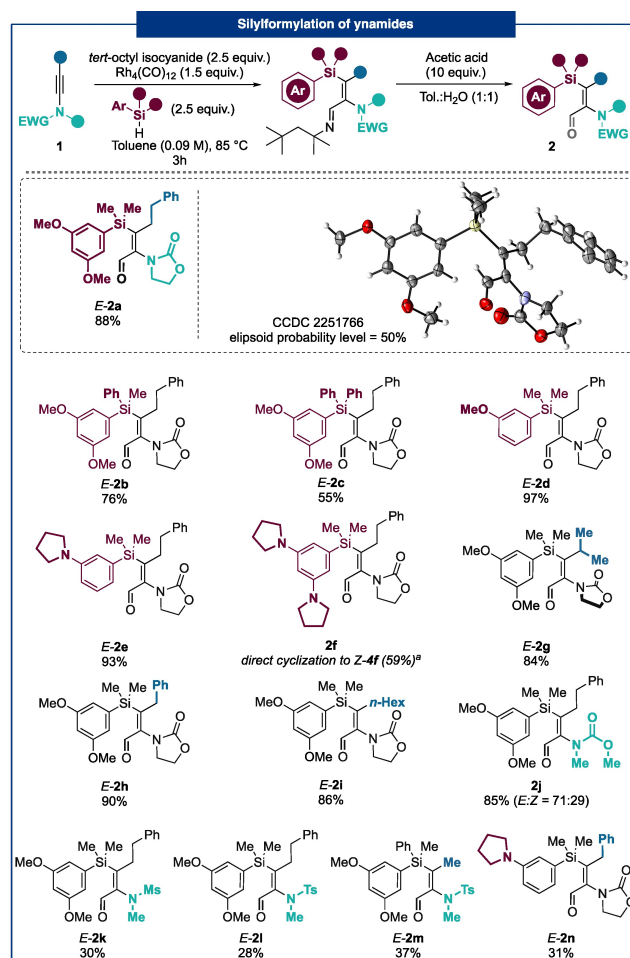
of Structure/Properties Relationship (including SAR) studies.

Based on our recent work on silylated captodative enamides,^[12] we have designed a two-step sequence starting from ynamides allowing a fast, selective, and diversified access to 3-amidobenzo[*b*]siline scaffolds. The proposed strategy (Figure 1.c) involves a formal 3-component silylformylation^[13] step followed by a Friedel-Crafts-type cyclization^[14]/isomerizing dehydration domino sequence. Interestingly, this approach offers a particularly high level of molecular variation from readily available compounds (ynamides, arylsilanes). To our knowledge, this approach would represent the first synthesis of benzo[*b*]silines carrying a non-heteroaromatic nitrogen (*e.g.* pyrrole or pyrazole) in position 3, opening the door to other

specific reactivities such as binding to bioactive molecules or ligation to biomolecules, for instance.

Results and Discussion

If we planned to use the reaction conditions we recently developed,^[13] we had never applied them to silanes bearing an electron-rich aromatic ring. Notably, if the silylimination step proceeded in a similar way to what we had observed in the case of phenyldimethylsilane (1 regioisomer, 1 stereoisomer) as a partner (Figure 2), the subsequent hydrolysis step, leading to the formation of the targeted aldehyde, proved to be much trickier. In that case we observed an undesired isomerization of the C=C double bond leading to a significant amount of the non-cyclizing *Z* compound. To avoid this phenomenon, very precise hydrolysis conditions were determined, namely 10 equivalents of acetic acid in a 1:1 mixture of toluene and water with rigorous monitoring of the reaction progress over time.



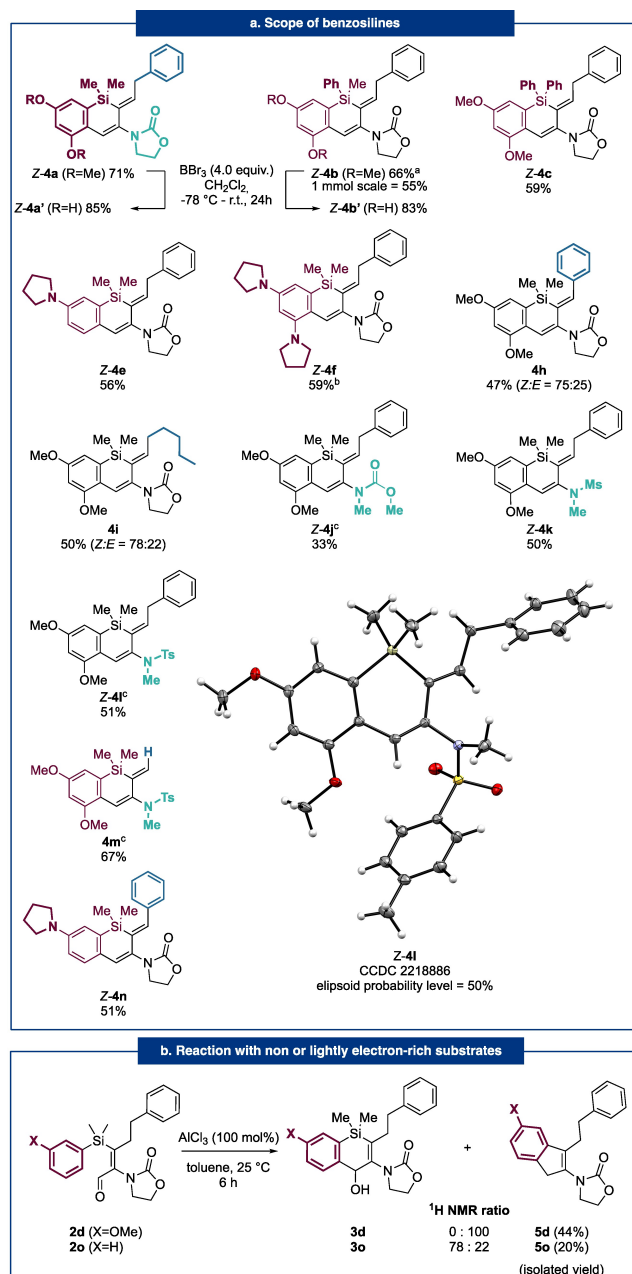
^{a)} See Figure 3.a for the structure of Z-4f.

Figure 2. Scope of the silylformylation of ynamides using electron-rich arylsilanes and X-ray-diffraction structure of **2a**.

Satisfactorily, once these conditions had been determined, the reaction proved to be tolerant to diverse variations (Figure 2) such as the nature of the silane (**2a–2f**), the distal ynamide chain (**2g–2i**) or nitrogen substitution (**2j–2m**). Interestingly, the silylformylation involving a more nucleophilic 1,3-dipyrrolidine-5-(dimethylsilyl)benzene led directly to the benzosiline-type product **Z-4f** (see structure Figure 3.a) upon acidic hydrolysis. It should be noted that a partial isomerization of the C=C double can be observed in the case of a Moc substituted ynamides (**2j**) and that yne-sulfonamides (**2k–2m**) led to the desired acroleins in lower yields of around 30–40%. Attempts to perform the silylformylation on aryl ynamides only led to the formation of hydrosilylated products while the ones on terminal ones led to a complete degradation of the starting material.

Once the 2-aminoacroleins were obtained, we optimized the Friedel-Crafts type cyclization to efficiently lead to the desired benzo[*b*]silines. While the addition reaction of an electron-rich aromatic ring to an aldehyde has been known for more than a century, here several specific challenges had to be addressed. The first one was related to the C=C isomerization problem already evoked previously during the hydrolysis of the imine intermediate. Indeed, the starting acroleins appear to be sensitive to acidic conditions and isomerization from the *E* to the *Z* configuration would make any cyclization impossible. The second relates to the potential sensitivity of vinylsilanes to the exposure to prolonged acidic conditions. Satisfyingly, after optimization of the reaction conditions (Table 1), we were able to cyclize stereoselectively acrolein **2a** to benzosilene **Z-4a**, after dehydration of intermediary benzosilanol **3a**, in a good 71% yield. Notably, 1 equivalent of Lewis acid was required to reach full conversion of the starting material while an excess of AlCl₃ (2 equiv.) led to a lower yield due to partial degradation of the product. To the best of our knowledge, this work represents the first example of intramolecular Friedel-Crafts cyclization on acrolein derivatives to form a 6-membered ring as well as the first one involving a subsequent isomerizing dehydration in a domino sequence. Remarkably, the reaction only led to a single stereoisomer of the *Z*-configuration product **4a** most probably due to allylic strain.^[15]

Surprisingly, cyclization of the mono methoxylated substrate *E*-**2d** (*meta* position) did not lead to the targeted benzosilene but to an indene **5d** (44%, Figure 3.b) that could result from a Salvadori-type rearrangement^[15] (see Figure 4 and related paragraph for mechanistic consideration). Once the optimized conditions were in hand, we explored the scope of this cyclization (Figure 3.a). To begin with, it appeared that the nature of the substituent on the silicon, other than the cyclizing aromatic ring, has relatively little influence on the efficiency or the selectivity of the




Cyclization conditions: AlCl₃ (100 mol%) in toluene at a concentration of 5.10⁻² M for 6h at 25 °C; ^a) 55% yield when performed on 1 mmol scale; ^b) The cyclization took place directly, without addition of AlCl₃, during the hydrolysis of the imine to form the acrolein *E*-**2j**, see Figure 2; ^c) 200 mol% of AlCl₃ at 70 °C during 24 h were required to obtain a complete conversion.

Figure 3. Scope of the cyclization leading to 3-amidobenzo[*b*]silines.

reaction (**Z-4a**, **Z-4b** and **Z-4c**). Off note, reactions of **4a** and **4b** with BBr₃ led efficiently to the corresponding hydroxyphenols **4a'** and **4b'**.

Table 1. Deviation from optimized conditions of the Friedel-Crafts cyclization.



Entry	Deviation	Conv. (%)	Yield 4 a (%)
1	none	100	71
2	BiCl ₃ as acid	100	59
3	Sc(OTf) ₃ or TfOH as acid	100	0
4	BF ₃ ·Et ₂ O or CSA as acid	0	-
5	AlCl ₃ (50 mol%)	80	38
6	AlCl ₃ (200 mol%)	100	29
7	CH ₂ Cl ₂ as solvent	80	53

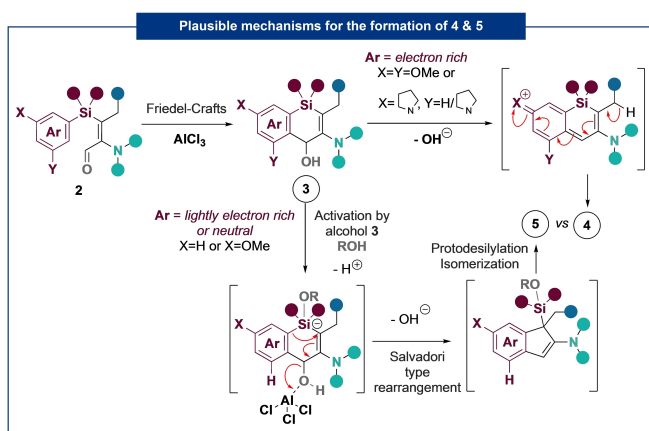


Figure 4. Proposed mechanisms for the formation of **4** and **5**.

Conversely, the mono pyrrolidine substrate *E*-**2e** cyclized to give the desired benzosililine *Z*-**4e** in 56% yield, accompanied by 20% of the isomerization product *Z*-**2e**. The cyclization of acrolein *E*-**2g** involving a sterically hindered substrate bearing an isopropyl substituent on the C=C double bond did not react under standard conditions and only degradation could be obtained while using higher temperature or Lewis acid loading. Notably, it appeared that the nature of the substituent on position 3 of the starting acroleins **2** has a clear influence on the diastereoselectivity of the reaction with respect to the C=C double bond (erosion of the selectivity in the case of phenyl-substituted **4h** and pentyl-substituted **4i**). Nicely, the reaction revealed to be tolerant to various protecting groups on the nitrogen substitution on position 2 of acroleins **2** as the reaction proved to be equally effective with Moc (*Z*-**4j**), Ms (*Z*-**4k**) or Ts (*Z*-**4l**) groups. The synthesis of benzosililines with a terminal exocyclic alkene (**4m**, 67%). Conversely to what has been observed in the case of the dimethoxy substrate *Z*-**2h**, the analogous substrate **2n** substituted by a

pyrrolidine led to the targeted benzosililine *Z*-**4n** as a single stereoisomer. Notably, the transformation applied to a substrate bearing a phenyl-substituted silicon group (*E*-**2o**) led to a 78:22 mixture of the hydroxylated benzosililine **4o** (Figure 3.b), which did not undergo isomerizing dehydration, and the indene **5o**. Noteworthy, substrates bearing an amide group proved incompatible with this cyclization and led to a complex mixture. Altogether, the various observations made during the scope evaluation enabled us to propose, starting from a common benzosilolinol **3**, two divergent mechanisms for the formation of the benzosililines **4** on one side and the indenenes **5** on the other side (Figure 4):

- **Benzosililine (4) pathway:** Knowing that when the aromatic ring is not electron-rich, benzosilolinol **3** can be identified, it seems likely that, in the case of an electron-rich aromatic silicon-substituent, a dearomatization induces the dehydration which is then followed by a re-aromatizing isomerization leading almost exclusively to the diastereomer *Z* (allylic strain).
- **Indene (5) pathway:** Starting with benzosilolinol **3**, the silicon atom could be activated by another alcohol **3** to form a hypercoordinated intermediate that could subsequently rearrange to transfer the electron rich aromatic ring *via* a dehydroxylating S_N^{2'} type reaction to form a silylated indene (Salvadori-type rearrangement^[15]). Finally, a proto-desilylation/isomerization sequence could lead to the product **5**.

In recent years, as mentioned previously, replacing the central oxygen atom of fluorescein and rhodamine by a silicon atom has become very popular as it can dramatically modulate the fluorescence properties of these valuable bioimaging probes.^[3] So, logically, we then evaluated the photophysical properties of these new benzo[*b*]sililines (Figure 1). First and foremost, preliminary investigations pointed out that no fluorescence could be observed for the silylated acroleins **2**. As another control, we also examined the silicon atom influence on the fluorescence of silacycles **4** by carrying out a proto-desilylation of compound **4a**. This reaction, promoted by TBAF in THF, led to the desired product **6a** in 58% yield without isomerization of the formerly exocyclic C=C double bond. As anticipated, the resulting product **6a** no longer exhibited detectable luminescence (Figure 5).

The photophysical properties of silacycles **4** were then evaluated by UV-Vis absorption and fluorescence spectroscopy in 1,2-dichloroethane. Compound **4a** showed a maximum absorbance at a wavelength of 358 nm for a maximum fluorescence emission at a wavelength of 428 nm resulting in an interesting Δ_{em-abs} of 70 nm (Stokes shift of 0.57 eV) (Figure 6 and Table 2). The quantum yield (Φ_F) on its side, indirectly measured using Rhodamine 6G as standard,^[17] appeared particularly modest with a value of 2%. Note

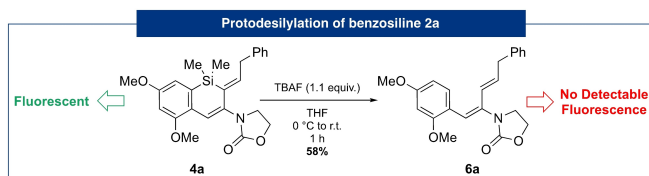
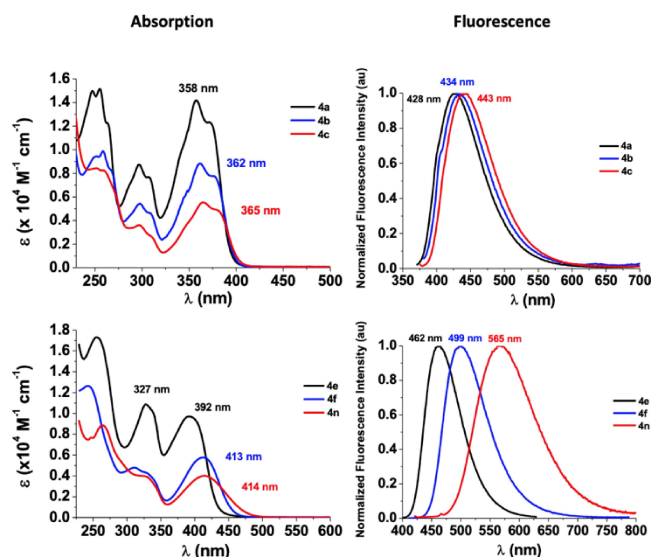


Figure 5. Critical influence of the silicon atom in the fluorescence of benzosilene derivative **4a**.



a) Measured in 1,2-DCE, $C=(1.10^{-6} - 1.10^{-5})$ M.

Figure 6. UV-Vis absorption and fluorescence spectra of representative benzosilenes **4**.

that replacing the methyl substituents on the silicon atom with one (**4b**) or two (**4c**) phenyl groups had very little influence on the quantum yields of fluorescence (similar Φ_F around 2%). However, these modifications resulted in a significant decrease of the molar absorption coefficients (approx. twofold reduction in intensity between **4a** and **4c**) and a slight bathochromic shift in the maximum absorption and fluorescence wavelengths ($\lambda_{\text{abs}}4c - \lambda_{\text{abs}}4a = 8$ nm; $\lambda_{\text{em}}4c - \lambda_{\text{em}}4a = 15$ nm).

Interestingly, when the benzosilene aromatic ring is substituted by a pyrrolidine in position 7 (**4e**), in comparison to **4a** substituted by two methoxy groups in position 5 and 7, shifts of 33 nm in absorption and 34 nm in emission are observed. Even more interestingly, the quantum yield of **4e** was measured more than 30 times higher (72%) than in **4a**. Notably, the addition of a second pyrrolidine in position 5 on the aromatic ring of benzosilene (**4f**) led to a significant bathochromic shift in both the absorption and emission wavelengths compared with compound **4e** and the $\Delta_{\text{em-abs}}$ was increased by 14 nm. However, the molar extinction coefficient was 2-fold lower, and the

quantum yield was measured at 63%. A study of the solvent effect on the photophysical properties of **4e** and **4f** has shown that solubilization in aprotic solvents of different polarities has virtually no impact on the absorption wavelength and slightly on the molar extinction coefficient. Nevertheless, the Stokes shift was found to increase significantly with increasing solvent polarity. Then we observed that the nature of the electron-withdrawing group (Moc **4j** or tosyl **4l**) on the nitrogen in position 3 of the benzosilenes has very little impact on absorption and emission properties (similar values to those of **4a**). Interestingly, if a benzosilene bearing an unsubstituted exocyclic C=C double bond (**4m**) appeared to have similar ϵ , λ_{abs} and λ_{em} to those substituted with an alkyl chain (**4i**), Φ_F was twice as high (2% vs 5%) demonstrating that alkyl substitution has a negative effect on the radiative process. Finally, the substitution of the exocyclic C=C double bond with a phenyl group (**4n**) significantly impacted both the absorption and the emission properties in comparison to those of the alkyl-substituted analog (**4e**). Indeed, a 23 nm bathochromic shift in the lowest-energy absorption band could be observed, as well as a 2-fold drop in molar extinction coefficient. In addition, we observed a significant broadening of both the absorption and the emission bands of fluorescence. Under photoexcitation, in 1,2-DCE, at the absorption maximum of the lowest-energy band, an emission band centered at 565 nm with a quantum yield measured at 26% indicated a particularly high $\Delta_{\text{em-abs}}$ of 152 nm (Stokes shift=0.81 eV). A study of the effect of solvent on the physicochemical properties of **4n** revealed, similarly to what has been observed for **4e** and **4f**, a bathochromic shift in the emission band correlated with increasing solvent polarity. As the absorption wavelength remained roughly similar, this phenomenon induces a significant increase in the $\Delta_{\text{em-abs}}$ up to a remarkable 166 nm (Stokes shift=0.88 eV) in acetonitrile. Altogether, this study shows that light structural modifications of the benzosilene scaffold lead to valuable modulation of the emission properties (Figure 7).

To gain a better understanding of the influence of substitutions of these benzo[*b*]silenes on their photophysical properties, we analyzed the absorption and emission properties of selected compounds using Density Functional Theory (DFT) and Time Dependent-DFT (see Computational Details section and Supporting Information for details). In particular, we focused on compounds **4a**, **4e**, **4f**, **4h** and **4n** to understand the nature of the electronic transitions responsible for the observed photophysical behavior and the influence of the substituents both on their energy and intensity.

In agreement with the experimental data, all the compounds in 1,2-DCE show a rather intense absorption (as can be seen from the computed oscillator

Table 2. Photophysical properties of selected 3-amidobenzo[*b*]silines.

Z-4	Solvent (polarity) ^[a]	λ_{abs} (nm) ^[b]	ϵ ($\times 10^4 \text{ M}^{-1} \text{ cm}^{-1}$)	λ_{em} (nm) ^[b]	Stokes Shift (ev)	Φ_{F} ^[c] (%)
4a	1,2-DCE (0.327)	358	1.4	428	0.57	2
4b	1,2-DCE (0.327)	362	0.9	434	0.57	2
4c	1,2-DCE (0.327)	365	0.6	443	0.60	2
4e	Toluene (0.099)	391	1.1	453	0.43	57
	1,2-DCE (0.327)	391	1.0	462	0.49	72
	CH ₃ CN (0.460)	393	1.0	469	0.51	64
4f	Toluene (0.099)	410	0.7	490	0.49	58
	1,2-DCE (0.327)	414	0.6	499	0.51	63
	CH ₃ CN (0.460)	409	0.8	501	0.56	49
4j	1,2-DCE (0.327)	356	0.9	420	0.53	n.d. ^[d]
4l	1,2-DCE (0.327)	357	1.5	414	0.48	2
4m	1,2-DCE (0.327)	355	1.4	414	0.50	5
4n	Toluene (0.099)	414	0.2	560	0.78	17
	1,2-DCE (0.327)	413	0.4	565	0.81	26
	CH ₃ CN (0.460)	409	0.3	575	0.88	20

^[a] Normalized solvent polarity E_{T}^{N} using water and TMS as extreme references.^[18]

^[b] λ refers to the wavelength of maximum absorption or emission, measured in 1,2-DCE, $C = (1.10^{-6} - 1.10^{-5}) \text{ M}$.

^[c] Relative quantum yields using Rhodamine 6G as reference.

^[d] Quantum yield too low to be accurately measured.

strengths, f , Table 3) in the visible range. The observed band originates from a single $S_0 \rightarrow S_1$ electronic transition of dominant HOMO-LUMO character. Analysis of the Natural Transition Orbitals involved (Figure 8) and of the associated Charge Transfer character (measured by the means of the D_{CT} index, Table 3) demonstrate how for all compounds this transition is of π - π^* character and largely involving delocalization over the C–C single-double network extending over the benzo[*b*]siline ring. No significant delocalization of both NTOs involved is instead observed on the nitrogen-containing substituent in position 3 which is consistent with the little dependence of absorption (and

emission) experimentally observed on the nature of the electron-withdrawing group on the nitrogen in position 3. On the other hand, donor groups present in positions 5 and 7, sizably contribute as donors (as demonstrated by their large contribution to the NTOs) thus explaining the observed redshift in absorption between compounds 4e and 4f. More interestingly, the possibility of extending the single-double bond length alternation (and conjugation) network with substituents such as the tosyl group acting as acceptor, significantly red shifts both absorption and emission of the compounds with respect to analogues substituted with alkyl chains. This is clear comparing the results

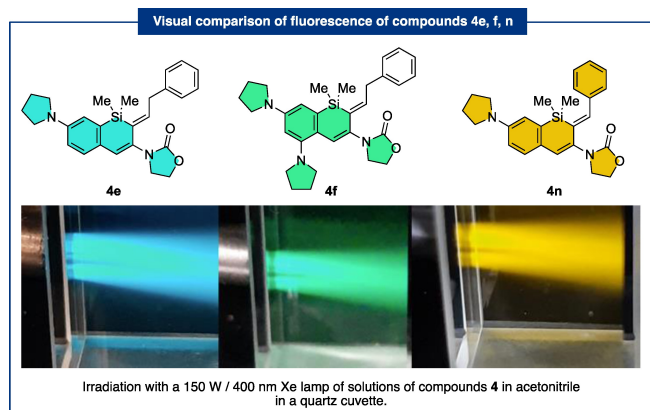


Figure 7. Visual comparison of irradiated (400 nm/150 W) solutions in acetonitrile of compounds **4e**, **4f** and **4n**.

Table 3. Photophysical properties computed for selected 3-amidobenzo[*b*]silines in 1,2 DCE at the PBE0 level using the 6-311 + G(d,p) basis set.

Z-4	λ_{abs} (nm)	f (a.u)	D_{CT} (Å)	λ_{em} (nm) ^[a]	Stokes shift (eV)
4a	368	0.62	1.99	463	0.70
4e	398	0.67	3.93	497	0.62
4f	422	0.64	3.04	533	0.61
4h	410	0.61	2.80	560	0.81
4n	446	0.63	4.41	611	0.75

^[a] Using the state-specific approach.

obtained for **4a** to those of **4h** or the results obtained for **4e** with respect to those of **4n**. Indeed, in the case of **4a** and **4e** the delocalization is limited to the exocyclic C=C bond (refer to Figure 8), while in **4h** and **4n** it extends up to the exocyclic C=C phenyl substituent thus significantly increasing the conjugation and the associated Charge Transfer (CT) character of the corresponding excited state. This effect can be clearly quantified comparing the excited state hole-electron separation as provided by the D_{CT} index. This index (Table 3) increases from 1.99 Å to 2.80 Å going from **4a** to **4h** and from 3.93 Å to 4.40 Å going from **4e** to **4n**. In other words, extending the single-double bond alternation out of the benzo[*b*]siline ring red shifts the absorption, increases the CT character and the Stokes shift. Not surprisingly, the compounds showing the largest CT are also those for which a larger solvatochromism is observed and computed (as reported in SI).

Interestingly a qualitative explanation of the observed emission quantum yield can also be given. Indeed, an increase of conjugation of substituents of the benzo[*b*]siline is expected to decrease the efficiency of non-radiative channels occurring via vibra-

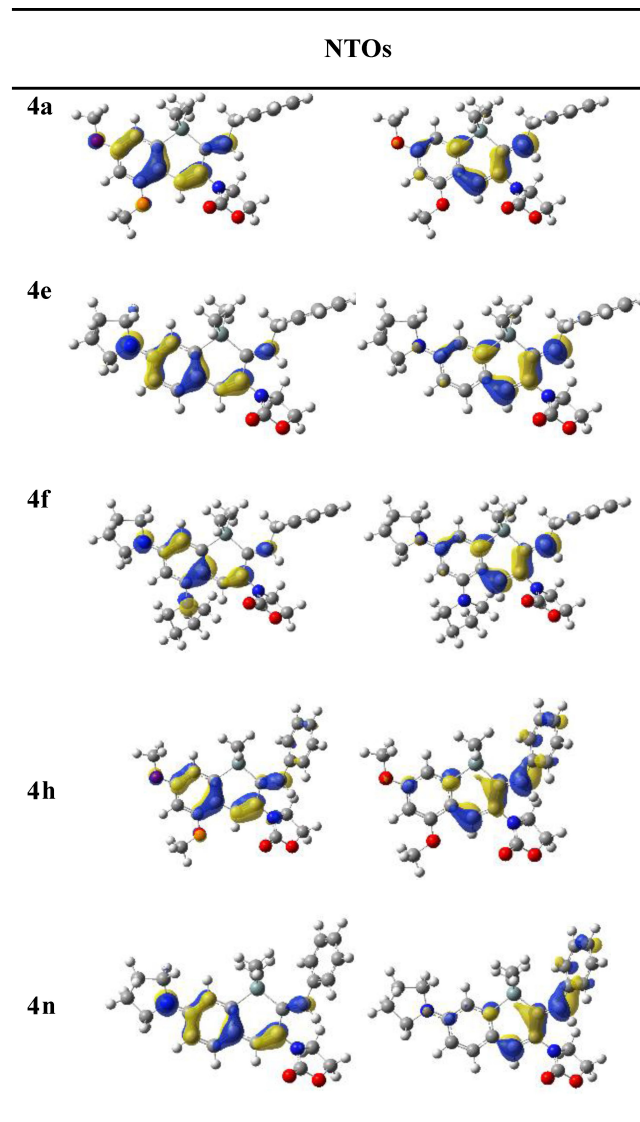


Figure 8. Graphical representation of computed NTOs associated to the $S_0 \rightarrow S_1$ transition of **4a**, **4e**, **4f**, **4h** and **4n**.

tional relaxation and internal conversion. On the other hand, the addition of non-conjugated substituents which might have a positive impact on the energetic (*i.e.* red shift absorption and emission, increase the charge transfer character and thus the Stokes shift) is expected to also increase the efficiency of non-radiative relaxation pathways and thus to be detrimental for the quantum yield. This reasoning qualitatively explains why for molecules displaying a larger degree of conjugation at the excited state (such as **4h** and **4n** with respect to **4a** and **4e**) a higher quantum yield is observed and, on the opposite, why the 5,7 pyrrolidine di-substituted derivative (**4f**) a red-shifted absorption but a lower quantum yield are measured with respect to the 7 mono substituted analogue (**4e**).

Conclusion

In summary, we have developed a modular 2-step synthesis of various 3-Amido-benzo[*b*]silines. Most of these scaffolds fluoresced with quantum yields and Stokes shifts of up to 76% and 0.88 eV respectively. In addition, the emission wavelengths could be significantly modified by slight structural modifications and these photophysical properties were rationalized by computational TD-DFT studies. Overall, these silacyclic molecular scaffolds offer interesting prospects for applications such as bioimaging probes or OLED materials.

Experimental Section^[19]

General Procedure for 3-Component Silylformylation of Ynamides to form 3-silyl-2-Amidoacroleins (2)

In an oven-dried sealed tube under argon, Rh₄(CO)₁₂ (1.5 mol%) was dissolved in dry toluene (C=0.09 M) and isocyanide (2.5 equiv.) was added to the red solution. The mixture was stirred at room temperature for 5 min and the solution turned from dark red to yellow accompanied by the release of gas (bubbles). Then, ynamide (1.0 equiv.) and silane (2.5 equiv.) were added to the solution. The reaction mixture was placed in a heating mantle and stirred at 85 °C for 3 hours. After full consumption of the starting material (followed by TLC), the reaction was cooled down to room temperature. To hydrolyse the newly formed imine intermediate, water (same volume as the toluene used to set up the initial reaction) and acetic acid (10.0 equiv.) were added, and the reaction was stirred at room temperature for another 3 h. The organic layer was separated, and the aqueous layer was extracted twice with EtOAc. The combined organic layers were washed twice with water, dried over MgSO₄, filtered, and concentrated in vacuo. The crude product was purified by column chromatography on silica gel to afford the desired aldehyde.

(*E*)-3-(dimethyl(phenyl)silyl)-2-(2-oxooxazolidin-3-yl)-5-phenylpent-2-enal (2a)

Off white solid. **mp**: 79–82 °C (recrystallized from pentane). **TLC** R_f: 0.25 (Cyclohexane/EtOAc 70:30). **IR** (neat) ν_{\max} 3017, 2956, 1741, 1677, 1426, 1412, 1295, 1140, 1085, 1047, 1032, 827, 775, 736, 699, 531 cm⁻¹. **¹H NMR** (500 MHz, C₆D₆) δ 9.77 (s, 1H, CHO), 7.11–7.07 (m, 2H), 7.01 (ddd, *J*=6.2, 3.0, 1.7 Hz, 3H), 6.93 (d, *J*=2.3 Hz, 2H), 6.55 (t, *J*=2.3 Hz, 1H), 3.58 (t, *J*=7.8 Hz, 2H), 3.46 (s, 6H), 2.86 (t, *J*=7.9 Hz, 2H), 2.75 (ddd, *J*=8.5, 6.7, 1.3 Hz, 2H), 2.67 (dd, *J*=9.1, 6.5 Hz, 2H), 0.33 (s, 6H). **¹³C{¹H} NMR** (126 MHz, C₆D₆) δ 187.5, 165.4, 161.7 (2 C), 157.3, 144.0, 141.4, 139.8, 128.7 (2 C), 128.8 (2 C), 126.6, 111.7 (2 C), 102.5 (CAr), 62.5 (O-CH₂), 55.2 (x2, O-CH₃), 45.7 (N-CH₂), 36.5 (CH₂), 35.5 (CH₂), -0.1 (x2, Si-CH₃). **²⁹Si{¹H} NMR** (99 MHz, C₆D₆) δ -6.74. **HRMS (ESI-TOF) m/z** [M + Na⁺] Calcd for C₂₄H₂₉NO₅SiNa 462.1708; Found 462.1707.

General Procedure for Friedel-Crafts Cyclization of 3-silyl-2-amidoacroleins (2) to Form 3-amido-1,2-dihydrobenzo[*b*]silines (4)

In an oven-dried round bottom flask under argon, the 2-amidoacrolein **2** was dissolved in freshly distilled toluene (C=0.05 M) followed by the addition of AlCl₃ (100 mol%). The mixture was stirred 6 hours at room temperature. The reaction was quenched using a saturated solution of potassium sodium tartrate (Rochelle salt). The aqueous layer was washed twice with EtOAc. The combined organic layers were washed twice with brine, dried over MgSO₄, filtered, and concentrated to give the crude benzosilene **4** which was purified by flash column chromatography on silica gel (treated with Et₃N).

(*E*)-3-(5,7-Dimethoxy-1,1-dimethyl-2-(2-phenylethylidene)-1,2-dihydrobenzo[*b*]silin-3-yl)oxazolidin-2-one (4a)

Off white solid. **mp**: 88–91 °C. **TLC** R_f: 0.30 (Cyclohexane/EtOAc 70:30). **IR** (neat) ν_{\max} 2953, 1740, 1586, 1408, 1294, 1254, 1198, 1044, 837 cm⁻¹. **¹H NMR** (500 MHz, CDCl₃) δ 7.32 (t, *J*=7.4 Hz, 2H), 7.25–7.18 (m, 3H), 6.97 (s, 1H), 6.61 (d, *J*=2.4 Hz, 1H), 6.50 (t, *J*=7.8 Hz, 1H), 6.42 (d, *J*=2.4 Hz, 1H), 4.42–4.35 (m, 2H), 3.85 (s, 3H), 3.81 (s, 3H), 3.76 (m, 2H), 3.73 (d, *J*=7.8 Hz, 2H), 0.50 (s, 6H). **¹³C{¹H} NMR** (126 MHz, CDCl₃) δ 160.0, 157.0, 157.0, 141.2, 139.4, 136.8, 132.8, 130.4, 128.3 (2 C), 128.1 (2 C), 126.0, 122.5, 120.8, 109.3, 98.7, 61.5, 55.2, 55.0, 47.9, 38.0, 0.0 (2 C). **²⁹Si{¹H} NMR** (99 MHz, CDCl₃) δ -17.29. **HRMS (ESI-TOF) m/z** [M + Na⁺] Calcd for C₂₄H₂₇NO₄SiNa 444.1602; Found 444.1607.

Computational Details Section

In order to compute the photophysical properties of selected molecules, DFT and TD-DFT calculations were performed to describe ground and excited states, respectively. The Gaussian 16 package^[20] was employed for all calculations. The global hybrid PBE0 exchange-correlation functional^[21,22] as well as the range-separated hybrid functional (LC-PBE) were used.^[23] Results reported in the main text are those corresponding to the PBE0 calculations, while LC-PBE results are discussed in Supporting Information. The 6–311+G(d,p)^[24,25] all-electron basis set was used to describe all atoms. Solvent effects were included implicitly by the means of the conductor like polarizable continuum model (CPCM).^[26,28] A state-specific formalism was applied to describe excited states relaxation. For structural optimizations, the default force and energy thresholds were applied as convergence criteria. Analysis of the excited states was performed using the Natural Transition Orbitals^[29] while their charge transfer character has been evaluated using the density based D_{CT} descriptor.^[30]

Acknowledgements

M.D. is grateful to the French National Agency of Research (ANR) for the grant allocated to this project including a PhD fellowship for S.G. (C-Sil, ANR-CE07-190016). The authors thank the CNRS and the University of Strasbourg for financial

support. T.Y. acknowledges a PhD grant from China Scholarship Council (CSC). The authors are grateful to Dr. Gilles Ulrich from ICPEES (University of Strasbourg) for his advice and for giving access to his specific device for quantum yield measurements. Dr. Mourad Elhabiri (LIMA UMR7042 CNRS-Unistra-UHA) is warmly thanked for fruitful discussions about the study of photophysical properties carried out during this work. The authors thank Dr. E. Wasielewski and M. Chessé, respective managers of the NMR and Analytical platforms of the department (LIMA UMR7042 CNRS-Unistra-UHA), for technical support. We thank Nathalie Gruber (Uni. Strasbourg) and Corinne Bailly (Uni. Strasbourg) for X-Ray analyses.

References


- [1] For a recent review see: F. Chen, L. Liu, W. Zeng, *Front. Chem.* **2023**, *11*, 1200494.
- [2] For representative reviews see: a) N. F. Lazareva, I. M. Lazarev, *Russ. Chem. Bull.* **2015**, *64*, 1221–1232; b) R. Ramesh, D. S. Reddy, *J. Med. Chem.* **2018**, *61*, 3779–3798; c) J. Fotie, C. M. Matherne, J. E. Wroblewski, *Chem. Biol. Drug Des.* **2023**, *102*, 235–254.
- [3] For representative examples see: a) D. N. Rao, X. Ji, S. C. Miller, *Chem. Sci.* **2022**, *13*, 6081–6088; b) J. B. Grimm, T. A. Brown, A. N. Tkachuk, L. D. Lavis *ACS Cent. Sci.* **2017**, *3*, 975–977; c) T. Egawa, Y. Koide, K. Hanaoka, T. Komatsu, T. Terai, T. Nagano, *Chem. Commun.* **2011**, *47*, 4162–4164; d) Y. Koide, Y. Urano, K. Hanaoka, T. Terai, T. Nagano, *J. Am. Chem. Soc.* **2011**, *133*, 5680–5682; e) Q. A. Best, N. Sattenapally, D. J. Dyer, C. N. Scott, M. E. McCarroll, *J. Am. Chem. Soc.* **2013**, *135*, 13365–13370; f) M. Fu, Y. Xiao, X. Qian, D. Zhao, Y. Xu, *Chem. Commun.* **2008**, 1780–1782; g) Y. Koide, Y. Urano, K. Hanaoka, T. Terai, T. Nagano *ACS, Chem. Biol.* **2011**, *6*, 600–608.
- [4] Representative examples: a) C. H. S. Hitchcock, F. G. Mann, A. Vanterpool, *J. Chem. Soc.* **1957**, 4537–4546; b) K. Oita, H. Gilman, *J. Am. Chem. Soc.* **1957**, *79*, 339–342; c) M. Oba, Y. Kawahara, R. Yamada, H. Mizuta, K. Nishiyama, *J. Chem. Soc. Perkin Trans. 2* **1996**, 1843–1848; d) M. E. Lee, H. M. Cho, C. H. Kim, W. Ando *Organometallics* **2001**, *20*, 1472–1475.
- [5] a) N. Agenet, J.-H. Mirebeau, M. Petit, R. Thouvenot, V. Gandon, M. Malacria, C. Aubert, *Organometallics* **2007**, *26*, 819–830; b) Y. Qin, J. Han, C. Ju, D. Zhao, *Angew. Chem. Int. Ed.* **2020**, *59*, 8481–8485.
- [6] Y. Takeyama, K. Nozaki, K. Matsumoto, K. Oshima, K. Utimoto, *Bull. Chem. Soc. Jpn.* **1991**, *64*, 1461–1466.
- [7] For a recent review on silacyclobutanes ring enlargements see: J. Huang, F. Liu, X. Wu, J.-Q. Chen, J. Wu, *Org. Chem. Front.* **2022**, *9*, 2840–2855.
- [8] S. Yoshioka, Y. Fujii, H. Tsujino, T. Uno, H. Fujioka, M. Arisawa, *Chem. Commun.* **2017**, *53*, 5970–5973.
- [9] Y. Liang, W. Geng, J. Wei, K. Ouyang, Z. Xi, *Org. Biomol. Chem.* **2012**, *10*, 1537–1542.
- [10] Z. Tan, F. Chen, G. Huang, Y. Li, H. Jiang, W. Zeng, *Org. Lett.* **2023**, *25*, 2846–2851.
- [11] M. Ahmad, A.-C. Gaumont, M. Durandetti, J. Maddaluno, *Angew. Chem. Int. Ed.* **2017**, *56*, 2464–2468.
- [12] a) P. Wagner, M. Donnard, N. Girard, *Org. Lett.* **2019**, *21*, 8861–8866 ; b) P. Hansjacob, F. R. Leroux, V. Gandon, M. Donnard, *Angew. Chem. Int. Ed.* **2022**, *61*, e202200204; c) P. Hansjacob, F. R. Leroux, M. Donnard, *Chem. Eur. J.* **2023**, e202300120; d) S. Golling, P. Hansjacob, N. Bami, F. R. Leroux, M. Donnard, *J. Org. Chem.* **2022**, *87*, 16860–16866; e) P. Hansjacob, C. Schwoerer, F. R. Leroux, M. Donnard, *Org. Biomol. Chem.* **2024**, *22*, 70–75.
- [13] S. Golling, F. R. Leroux, M. Donnard, *Org. Lett.* **2021**, *23*, 8093–8097.
- [14] D. Wittenberg, P. B. Talukdar, H. Gilman, *J. Am. Chem. Soc.* **1960**, *82*, 3608–3610.
- [15] R. W. Hoffmann, *Chem. Rev.* **1989**, *89*, 1841–1860.
- [16] L. A. Aronica, P. Raffa, A. M. Caporusso, P. Salvadori, *J. Org. Chem.* **2003**, *68*, 9292–9298.
- [17] A. M. Brouwer, *Pure Appl. Chem.* **2011**, *83*, 2213–2228.
- [18] C. Reichardt, T. Welton, *Solvents and Solvent Effects in Organic Chemistry*, Wiley-VCH Verlag GmbH & Co. KGaA: Weinheim, Germany, **2010**.
- [19] CCDC-2251766 and CCDC-2218886 contain the supplementary crystallographic data for compound **2a** and **4I** respectively. These data can be obtained free of charge from The Cambridge Crystallographic Data Centre via www.ccdc.cam.ac.uk/structures.
- [20] R. C. Gaussian 16, M. J. Frisch, G. W. Trucks, H. B. Schlegel, G. E. Scuseria, M. A. Robb, J. R. Cheeseman, G. Scalmani, V. Barone, G. A. Petersson, H. Nakatsuji, X. Li, M. Caricato, A. V. Marenich, J. Bloino, B. G. Janesko, R. Gomperts, B. Mennucci, H. P. Hratchian, J. V. Ortiz, A. F. Izmaylov, J. L. Sonnenberg, D. Williams-Young, F. Ding, F. Lipparini, F. Egidi, J. Goings, B. Peng, A. Petrone, T. Henderson, D. Ranasinghe, V. G. Zakrzewski, J. Gao, N. Rega, G. Zheng, W. Liang, M. Hada, M. Ehara, K. Toyota, R. Fukuda, J. Hasegawa, M. Ishida, T. Nakajima, Y. Honda, O. Kitao, H. Nakai, T. Vreven, K. Throssell, J. A. Montgomery, Jr., J. E. Peralta, F. Ogliaro, M. J. Bearpark, J. J. Heyd, E. N. Brothers, K. N. Kudin, V. N. Staroverov, T. A. Keith, R. Kobayashi, J. Normand, K. Raghavachari, A. P. Rendell, J. C. Burant, S. S. Iyengar, J. Tomasi, M. Cossi, J. M. Millam, M. Klene, C. Adamo, R. Cammi, J. W. Ochterski, R. L. Martin, K. Morokuma, O. Farkas, J. B. Foresman, D. J. Fox, Gaussian, Inc., Wallingford CT, **2019**.
- [21] C. Adamo, V. Barone, *J. Chem. Phys.* **1999**, *110*, 6158–6170.
- [22] M. Ernzerhof, G. E. Scuseria, *J. Chem. Phys.* **1999**, *110*, 5029–5036.
- [23] H. Iikura, T. Tsuneda, T. Yanai, K. Hirao, *J. Chem. Phys.* **2001**, *115*, 3540–3544.
- [24] R. Krishnan, J. S. Binkley, R. Seeger, J. A. Pople, *J. Chem. Phys.* **2008**, *72*, 650–654.
- [25] T. Clark, J. Chandrasekhar, G. W. Spitznagel, P. V. R. Schleyer, *J. Comb. Chem.* **1983**, *4*, 294–301.
- [26] S. Miertuš, E. Scrocco, J. Tomasi, *Chem. Phys.* **1981**, *55*, 117–129.

- [27] V. Barone, M. Cossi, *J. Phys. Chem. A* **1998**, *102*, 1995–2001
- [28] M. Cossi, N. Rega, G. Scalmani, V. Barone, *J. Comb. Chem.* **2003**, *24*, 669–81.
- [29] R. L. Martin, *J. Chem. Phys.* **2003**, *118*, 4775–77.
- [30] T. Le Bahers, C. Adamo, I. Ciofini, *J. Chem. Theory Comput.* **2011**, *7*, 2498–2506.
-

RESEARCH ARTICLE

3-Amido-benzo[*b*]silines: Straightforward Modular 2-Step Synthesis and Photophysical Properties

Adv. Synth. Catal. **2024**, *366*, 1–11

 Dr. S. Golling, T. Yan, Dr. V. Mazan, Dr. F. R. Leroux, Dr. I. Ciofini, Dr. M. Donnard*

